



## Comparative investigation of photo- and thermal-oxidation processes in poly(butylene terephthalate)

S. Carroccio\*, P. Rizzarelli, G. Scaltro, C. Puglisi

Istituto di Chimica e Tecnologia dei Polimeri – Consiglio Nazionale delle Ricerche, V. le A. Doria 6 – 95125 Catania, Italy

### ARTICLE INFO

#### Article history:

Received 29 October 2007  
Received in revised form 4 May 2008  
Accepted 11 May 2008  
Available online 15 May 2008

#### Keywords:

Poly(1,4-butylene terephthalate)  
Thermal-oxidation  
Photo-oxidation

### ABSTRACT

Thermal- and photo-oxidation processes occurring in poly(1,4-butylene terephthalate) (PBT) were investigated and compared in order to find out potential dissimilarities in the oxidation pathways of this polymer. The oxidized compounds were analyzed by matrix assisted laser desorption ionization-time of flight mass spectrometry (MALDI-TOF MS). Applications of MALDI to the study of polymer photo- and thermo-oxidation are quite recent and involve the collection of MALDI spectra at different irradiation times and/or temperatures to observe the structural changes induced by heat or light under an oxidizing atmosphere. The polymer sample can be directly analyzed and the recorded MALDI spectrum arises from a mixture of non-oxidized and oxidized chains. The results obtained by MALDI are highly informative, as compared with previous studies based on conventional techniques, yielding precise information on the size, structure, and end groups of molecules derived from the oxidation process.

According to the structure of the compounds identified in this work, two thermal-oxidation processes and two photo-oxidation cleavages have been unambiguously ascertained to occur in PBT. Furthermore, the inspection of the data acquired by MALDI allowed discriminating the degradation mechanisms entirely induced by light or heat without the involvement of oxygen.

© 2008 Elsevier Ltd. All rights reserved.

### 1. Introduction

Poly(1,4-butylene terephthalate) (PBT) is an engineering plastic with a good balance of mechanical and electrical properties widely used in automobile components such as connectors. However, it is well known that at the processing temperature (250–280 °C) thermal, oxidative and hydrolytic degradation may take place [1]. Furthermore, PBT is progressively degraded, depending on the temperature and the outdoor applications, by thermo- and photo-oxidative reactions that arise during its lifetime. Therefore, the understanding of chemical degradation reaction is necessary to prevent these undesirable processes.

The chemistry of thermal, thermo- and photo-oxidation reactions that occur in aromatic polyesters has been studied extensively in the past [1–7]. It is well established in the literature [1,7] that a  $\beta$ -CH hydrogen transfer is involved in the thermal degradation process, leading to the formation of oligomers with carboxylic and olefin end groups. The mechanisms of thermo- and photo-degradation are obviously complicated by the contribution of oxygen and they have mainly been studied for many years by UV, IR and wet chemistry methods, to follow the process and to identify the

products formed [2,3], frequently with the support of model compounds [6,7]. Bothelo et al. [6] carried out a comparative study on thermal- and thermo-oxidative degradation of PET and PBT with their respective model compounds. On the basis of the products identified by GC-MS, they accomplished that the thermo-oxidation mechanism involves oxidation at the  $\alpha$ -methylene carbon with the formation of peroxides. The consecutive chain scission produces aromatic and aliphatic acids, anhydrides and alcohols. Rivaton et al. [2,3] studied photolysis and photo-oxidation mechanisms of PBT by using UV and FT-IR, coupled with chemical derivatization reactions. According to the photo-oxidation products identified they deduced that photolytic reactions have a dominant effect with respect to the photo-oxidative degradation occurred in  $\alpha$ -methylene carbon.

However, UV and IR techniques supply structural information only on functional groups or segments of molecules, not on the entire molecule. These techniques might therefore prove inadequate in providing exhaustive information on the molecular structure of the complex mixture of compounds present in thermo- and photo-oxidized polymer samples. Additionally, molecules formed in oxidation processes are often very reactive, do not accumulate, and are present only in minor amounts among the reaction products requiring a high sensitivity to be monitored.

In the last decade the analysis of polymers has taken advantage from the development of matrix assisted laser desorption ionization-time of flight MS (MALDI-TOF MS), a highly sensitive,

\* Corresponding author. Tel.: +39 (0) 95 339926; fax: +39 (0) 95 221541.  
E-mail address: [scarroccio@unict.it](mailto:scarroccio@unict.it) (S. Carroccio).

nonaveraging technique that allows the direct determination of the individual molecules contained in a polymer sample [8,9]. Applications of MALDI to the study of polymer photo- and thermo-oxidation are quite recent [10–16] and involve the collection of MALDI spectra at different irradiation times and/or temperature to observe the structural changes induced by heat or light under an oxidizing atmosphere. The polymer sample can be directly analyzed and the recorded MALDI spectrum arises from a mixture of non-oxidized and oxidized chains. The results obtained for the systems so far investigated by MALDI [10–16] are remarkably highly informative, in comparison with previous studies based on conventional techniques, yielding precise information on the size, structure and end groups of molecules originated in the oxidation process.

In the present work, we report a comparative study of the thermo-oxidation and photo-chemical behaviour of poly(1,4-butylene terephthalate). PBT films were subjected to thermo- and photo-aging and the nature of the oxidation products and the mechanisms involved were analyzed by a fast and highly sensitive technique such as matrix assisted laser desorption ionization-time of flight mass spectrometry (MALDI-TOF MS). According to the structure of the compounds identified in this work, two thermal-oxidation processes and two photo-oxidation cleavages have been unambiguously ascertained to occur in PBT. Furthermore, the inspection of the data acquired by MALDI allowed discriminating the degradation mechanisms entirely induced by light or heat without the involvement of oxygen. Detailed structural information are described and compared.

## 2. Experimental section

### 2.1. Materials

Basic materials were purchased from Sigma–Aldrich Chemical Co. (Milan, Italy). Poly(1,4-butylene terephthalate) ( $M_v = 29,310$  Da) and 2-(4-hydroxyphenylazo)benzoic acid (HABA) were used as supplied.

### 2.2. Films preparation and thermo-oxidation procedure

PBT solution (250  $\mu$ L, 5% in 1,1,1,3,3,3-hexafluoro-2-propanol) (HFIP) were placed in glass vessels and dried at room temperature up to complete solvent evaporation. The thin films, formed by casting on the wall of the glass vessel, were thermo-oxidized at 250 and 280 °C in atmospheric air for 15, 30, 60, 120 and 180 min. The soluble part of the thermo-oxidized samples was analyzed by viscometry and MALDI-TOF MS. At least two separate films were analyzed at each exposure time.

### 2.3. Films preparation and photo-oxidative procedure

Photo-oxidation was performed on films of PBT obtained by solvent casting from a 5% HFIP solution. Photo-oxidative degradation of PBT samples was carried out on a QUV PANEL apparatus at 70 °C, with continued exposure to UV radiation (UVA 340 lamps) for up to 168 h. The soluble part of the photo-oxidized samples was analyzed by viscometry and MALDI-TOF MS. At least two different films were analyzed at each exposure time.

### 2.4. MALDI-TOF MS analysis

Matrix assisted laser desorption ionization-time of flight (MALDI-TOF) mass spectra were recorded in reflector mode using a Voyager-DE STR (Applied Biosystems) mass spectrometer equipped with a nitrogen laser emitting at 337 nm with a 3-ns pulse width and working in positive ion mode. The accelerating voltage was set at 20 kV, the grid voltage and the delay time were optimized for each

sample to achieve the higher molar mass values. The laser irradiance was maintained slightly above threshold. 2-(4-Hydroxyphenylazo)-benzoic acid (HABA) (0.1 M in HFIP) was used as matrix.

Appropriate volumes of polymer solution (7 mg/mL in HFIP) and matrix solution were mixed in order to obtain a 2:1, 1:1 and 1:2 ratios (sample/matrix v/v). Each sample/matrix mixture (1  $\mu$ L) was spotted on the MALDI sample holder and slowly dried to allow matrix crystallization.

The resolution of the MALDI spectra reported in the text is about 7000 FWHM, and the accuracy of mass determination was about 80 ppm in the mass range of 1000–2000 Da and 250 ppm in the mass range of 2000–3000 Da.

To distinguish and separate between the contributions of isotopic peaks  $M + 1$  and  $M + 2$  and peaks due to isobaric structures, a deisotoping program (Data Explorer™ software) was used. This program produces a theoretical spectrum for each species and subtracts from the experimental spectrum the intensity calculated values of  $M + 1$  and  $M + 2$  isotopic peaks. Thus, the deisotoping spectrum shows only the first mass peak  $M$  for each species.

The structural identification of MALDI peaks in Table 1 was mainly made on the basis of empirical formulas. However, isotopic resolution helps considerably in the peak-assignment process through the comparison of the relative intensities of isotopic peaks corresponding to oligomers of increasing molar mass [10,15,16]. Some plausible structures were also derived from and supported by previous studies [1–7].

### 2.5. Viscometry

Molar mass values of photo- and thermo-oxidized PBT samples at 250 °C were calculated from viscosity measurements. The inherent viscosities were measured with an Ubbelohde viscometer at a concentration of 0.5 g/dL in phenol/tetrachloroethane 60/40 w/w, at  $30 \pm 0.1$  °C. The Mark–Houwink equation was used for PBT to calculate the  $M_v$  values ( $[\eta] = KM_v^a$ ,  $K = 14.5 \times 10^{-3}$ ;  $a = 0.82$ ) [1].

## 3. Results and discussion

A commercial PBT sample was used for this study. Thin PBT films, obtained by solvent casting in appropriate glassware, were subjected to thermo- and photo-oxidation procedure in atmospheric air. Thermal- and photo-oxidation processes occurring in polymer films were investigated and compared.

PBT film samples were photo-oxidized at 70 °C up to 168 h and the soluble part was analyzed by viscometry. The  $M_v$  change of photo-oxidized PBT films, reported in Fig. 1, shows a significant decrease in molar mass values after 72 h and at higher exposure times the  $M_v$  values level off.

PBT film samples were heated in atmospheric air at 250 and 280 °C up to 180 min. In these conditions, the thermo-oxidative process was fairly rapid producing a noticeable reduction of molar mass with the heating time, after few minutes (Fig. 1). In fact, after 7 min of thermo-oxidation at 250 °C, the  $M_v$  value decreases to about 70%. These data confirm that the entire PBT films were involved in the thermo-oxidation process. After 10 min the  $M_v$  value increases, reasonably as a consequence of crosslinking phenomena.

In order to identify the oxidation products, samples of thermo- and photo-oxidized films were taken at different degradation times and analyzed in duplicate by matrix assisted laser desorption ionization-time of flight mass spectrometry (MALDI-TOF MS). Table 1 lists the oligomer structures assigned to the ions appearing in the MALDI-TOF mass spectra of thermo- and photo-oxidized PBT samples, discussed below. The identification of the structure and end groups attached to the oligomers produced is of outmost importance, since the end groups may reveal the particular

mechanism that has been active in the oxidation process. However, the recorded MALDI spectrum arises from a mixture of non-oxidized and oxidized chains, therefore the thermo- and photo-oxidation were carried out on extremely thin polyester films (see the Section 2) to maximize the percentage of photo- and thermo-

oxidation products with respect to the non-oxidized chains in the bulk and get information about the degradation mechanisms.

The MALDI mass spectrum of the original PBT sample is reported in Fig. 2. The peaks belong to four different mass series, corresponding to sodiated macromolecular ions. At low molar masses,

**Table 1**

Structural assignments of ions appearing in the MALDI-TOF mass spectra of thermo- and photo-oxidized PBT samples

Symbols (degradation pathway)	Structures	<i>n</i>	MNa <sup>+</sup>	MK <sup>+</sup>
A (OS)		6	1343.4	
		12	2664	
		13	2884	
		14	3104	
A (β-H-transfer)		5	1343.4	
B (route 2)		5	1347.4	
C (OS)		6	1361.4	1377.4
		12	2682	
C (route 2)		5	1361.4	
A <sub>1</sub> (β-H-transfer)		5	1365.4	
D (route 2)		5	1375.4	
D (route 1)				
C <sub>1</sub> (OS)		6	1383.4	
E (route 2)		5	1387.4	
E (route 2)				
F (N I)		6	1389.4	
F (route 2)				

(continued on next page)

Table 1 (continued)

Symbols (degradation pathway)	Structures	n	MNa <sup>+</sup>	MK <sup>+</sup>
F (route 2)	$\text{HCOO} \left[ \text{CO} - \text{C}_6\text{H}_4 - \text{COO} - (\text{CH}_2)_4\text{O} \right]_n \text{CO} - \text{C}_6\text{H}_4 - \text{COO}(\text{CH}_2)_2\text{COOH}$	5	1389.4	
F (route 2)	$\text{CH}_3(\text{CH}_2)_2\text{O} \left[ \text{CO} - \text{C}_6\text{H}_4 - \text{COO} - (\text{CH}_2)_4\text{O} \right]_n \text{CO} - \text{C}_6\text{H}_4 - \text{COO}(\text{CH}_2)_3\text{OH}$			
D <sub>1</sub> (route 1)	$\text{Na}^+ \text{O}^- \left[ \text{CO} - \text{C}_6\text{H}_4 - \text{COO} - (\text{CH}_2)_4\text{O} \right]_n \text{CO} - \text{C}_6\text{H}_4 - \text{COO}(\text{CH}_2)_3\text{COOH}$	5	1397.4	
G (β-H-transfer)	$\text{H}_2\text{C}=\text{CH}(\text{CH}_2)_2\text{O} \left[ \text{CO} - \text{C}_6\text{H}_4 - \text{COO} - (\text{CH}_2)_4\text{O} \right]_n \text{H}$	6	1415.5	
D <sub>2</sub> (route 1)	$\text{Na}^+ \text{O}^- \left[ \text{CO} - \text{C}_6\text{H}_4 - \text{COO} - (\text{CH}_2)_4\text{O} \right]_n \text{CO} - \text{C}_6\text{H}_4 - \text{COO}(\text{CH}_2)_3\text{COO}^- \text{Na}^+$	5	1419.4	
H (route 1–2)	$\text{HOOC}(\text{CH}_2)_3\text{O} \left[ \text{CO} - \text{C}_6\text{H}_4 - \text{COO} - (\text{CH}_2)_4\text{O} \right]_n \text{CO} - \text{C}_6\text{H}_4 - \text{COO}(\text{CH}_2)_2\text{CHO}$	5	1431.5	
H (route 1)	$\text{HCO}(\text{CH}_2)_3\text{O} \left[ \text{CO} - \text{C}_6\text{H}_4 - \text{COO} - (\text{CH}_2)_4\text{O} \right]_n \text{H}$	6	1431.5	
I (OS)	$\text{HO}(\text{CH}_2)_4\text{O} \left[ \text{CO} - \text{C}_6\text{H}_4 - \text{COO} - (\text{CH}_2)_4\text{O} \right]_n \text{H}$	6 12 13	1433.5 2754 2974	
H <sub>1</sub> (route 1–2)	$\text{Na}^+ \text{OOC}(\text{CH}_2)_3\text{O} \left[ \text{CO} - \text{C}_6\text{H}_4 - \text{COO} - (\text{CH}_2)_4\text{O} \right]_n \text{CO} - \text{C}_6\text{H}_4 - \text{COO}(\text{CH}_2)_2\text{CHO}$	5	1233.4	
J (route 1)	$\text{HO} - \text{C}_6\text{H}_4 - \text{COO}(\text{CH}_2)_4\text{O} \left[ \text{CO} - \text{C}_6\text{H}_4 - \text{COO} - (\text{CH}_2)_4\text{O} \right]_n \text{CO} - \text{C}_6\text{H}_4 - \text{OH}$	4	1233.4	
J (CL)	$\text{HO} \left[ \text{CO} - \text{C}_6\text{H}_4 - \text{COO} - (\text{CH}_2)_4\text{O} \right]_n \text{CO} - \text{C}_6\text{H}_3(\text{COOH})_2$	5	1453.5	
K (route 1)	$\text{HO} \left[ \text{CO} - \text{C}_6\text{H}_4 - \text{COO} - (\text{CH}_2)_4\text{O} \right]_n \text{CO} - \text{C}_6\text{H}_5$	5	1245.4	
J <sub>1</sub> (CL)	$\text{HO} \left[ \text{CO} - \text{C}_6\text{H}_4 - \text{COO} - (\text{CH}_2)_4\text{O} \right]_n \text{CO} - \text{C}_6\text{H}_3(\text{COO}^- \text{Na}^+)_2$	4	1255.3	
L (route 1)	$\text{HO} \left[ \text{CO} - \text{C}_6\text{H}_4 - \text{COO} - (\text{CH}_2)_4\text{O} \right]_n \text{CO} - \text{C}_6\text{H}_4 - \text{OH}$	5	1261.4	1277.4
M (CL)	$\text{HO} \left[ \text{CO} - \text{C}_6\text{H}_4 - \text{COO} - (\text{CH}_2)_4\text{O} \right]_n \text{CO} - \text{C}_6\text{H}_3(\text{COOH})_2$	4	1275.4	

Table 1 (continued)

Symbols (degradation pathway)	Structures	n	MNa <sup>+</sup>	MK <sup>+</sup>
J <sub>2</sub> (CL)	$\text{HO} \left[ \text{CO} - \text{C}_6\text{H}_4 - \text{COO} - (\text{CH}_2)_4\text{O} \right]_n \text{CO} - \text{C}_6\text{H}_3(\text{COO}^- \text{Na}^+)_2$	4	1277.3	
L <sub>1</sub> (route 1)	$\text{Na}^+ \text{O} \left[ \text{CO} - \text{C}_6\text{H}_4 - \text{COO} - (\text{CH}_2)_4\text{O} \right]_n \text{CO} - \text{C}_6\text{H}_4 - \text{OH}$	5	1283.4	
N (route 1–route 2)	$\text{HO} \left[ \text{CO} - \text{C}_6\text{H}_4 - \text{COO} - (\text{CH}_2)_4\text{O} \right]_n \text{CO} - \text{C}_6\text{H}_4 - \text{COOH}$	5	1289.4	1305.4
M <sub>1</sub> (CL)	$\text{HO} \left[ \text{CO} - \text{C}_6\text{H}_4 - \text{COO} - (\text{CH}_2)_4\text{O} \right]_n \text{CO} - \text{C}_6\text{H}_3(\text{COO}^- \text{Na}^+)_2 - \text{COO}(\text{CH}_2)_3\text{COOH}$	4	1297.4	
J <sub>3</sub> (CL)	$\text{Na}^+ \text{O} \left[ \text{CO} - \text{C}_6\text{H}_4 - \text{COO} - (\text{OCH}_2)_4\text{O} \right]_n \text{CO} - \text{C}_6\text{H}_3(\text{COO}^- \text{Na}^+)_2$	4	1299.3	
N <sub>1</sub> (route 1–route 2)	$\text{Na}^+ \text{O} \left[ \text{CO} - \text{C}_6\text{H}_4 - \text{COO} - (\text{CH}_2)_4\text{O} \right]_n \text{CO} - \text{C}_6\text{H}_4 - \text{COOH}$	5	1311.4	1327.4
O (OS)	$\text{CH}_3\text{O} \left[ \text{CO} - \text{C}_6\text{H}_4 - \text{COO} - (\text{CH}_2)_4\text{O} \right]_n \text{CO} - \text{C}_6\text{H}_4 - \text{COOCH}_3$	12 13	2858 3078	
M <sub>2</sub> (route 2–1)	$\text{HO}(\text{CH}_2)_2\text{O} \left[ \text{CO} - \text{C}_6\text{H}_4 - \text{COO} - (\text{CH}_2)_4\text{O} \right]_n \text{CO} - \text{C}_6\text{H}_4 - \text{OH}$	5	1319.4	
M <sub>2</sub> (CL)	$\text{HO} \left[ \text{CO} - \text{C}_6\text{H}_4 - \text{COO} - (\text{CH}_2)_4\text{O} \right]_n \text{CO} - \text{C}_6\text{H}_3(\text{COO}^- \text{Na}^+)_2 - \text{COO}(\text{CH}_2)_3\text{COO}^- \text{Na}^+$	4	1319.4	
M <sub>2</sub> (CL)	$\text{HO} \left[ \text{CO} - \text{C}_6\text{H}_4 - \text{COO} - (\text{CH}_2)_4\text{O} \right]_n \text{CO} - \text{C}_6\text{H}_3(\text{COOH})_2 - \text{COO}(\text{CH}_2)_3\text{COOH}$	4	1319.4	
N <sub>2</sub> (route 1–route 2)	$\text{Na}^+ \text{O} \left[ \text{CO} - \text{C}_6\text{H}_4 - \text{COO} - (\text{CH}_2)_4\text{O} \right]_n \text{CO} - \text{C}_6\text{H}_4 - \text{COO}^- \text{Na}^+$	5	1333.4	1349.3
N <sub>2</sub> (route 1)	$\text{HO}(\text{CH}_2)_4\text{O} \left[ \text{CO} - \text{C}_6\text{H}_4 - \text{COO} - (\text{CH}_2)_4\text{O} \right]_n \text{CO} - \text{C}_6\text{H}_4 - \text{OH}$			

(continued on next page)

Table 1 (continued)

Symbols (degradation pathway)	Structures	n	MNa <sup>+</sup>	MK <sup>+</sup>
M <sub>3</sub> (CL)	$\text{Na}^+ \text{O} \left[ \text{CO} - \text{C}_6\text{H}_4 - \text{COO} - (\text{CH}_2)_4 \text{O} \right]_n \text{CO} - \text{C}_6\text{H}_4 - \text{COO}^- \text{Na}^+$ $\text{C}_6\text{H}_4 - \text{COO}(\text{CH}_2)_3\text{COO}^- \text{Na}^+$	4	1341.4	
M <sub>3</sub> (CL)	$\text{HO} \left[ \text{CO} - \text{C}_6\text{H}_4 - \text{COO} - (\text{CH}_2)_4 \text{O} \right]_n \text{CO} - \text{C}_6\text{H}_4 - \text{COO}^- \text{Na}^+$ $\text{HOOC} - \text{C}_6\text{H}_4 - \text{COO}(\text{CH}_2)_3\text{COOH}$			
P (route 1)	$\text{HOCO}(\text{CH}_2)_3\text{O} \left[ \text{CO} - \text{C}_6\text{H}_4 - \text{COO} - (\text{CH}_2)_4 \text{O} \right]_n \text{H}$	6	1447.5	

OS = original sample; CL = cross-linking; "route 1–2" means that one end group is originated from route 1 and the other from route 2; "route 1–route 2" has been used for end groups that can derive from route 1 or route 2.

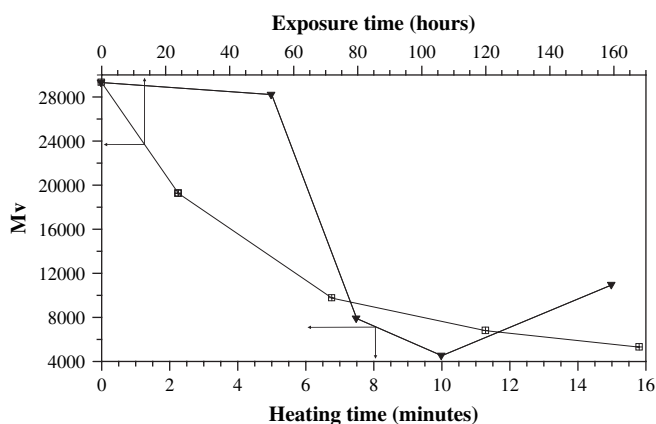


Fig. 1. Molar mass values of PBT samples thermo-oxidized at 250 °C (▼) and photo-oxidized at 70 °C (▣) as a function of the heating and exposure time.

the most abundant ions are due to cyclic oligomers at  $m/z$  2664 +  $n$ 220 (mass series A, Table 1), whereas at higher molar masses the most prominent peaks that appear at  $m/z$  2754 +  $n$ 220 (mass series I, Table 1), are assigned to oligomers with 1,4-butane-diol end groups at both chain ends. A third mass series, appearing in the inset of Fig. 2 at  $m/z$  2682, can be assigned to sodiated ions terminated with 1,4-butane-diol at one end and terephthalic acid at the other end (species C, Table 1). Macromolecular ions at  $m/z$  2858 bearing methyl ester groups as chain ends (mass series O, Table 1) are detected as well.

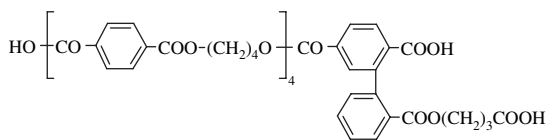
The MALDI mass spectrum of the original PBT sample (Fig. 2) evidences a preferential production of cyclic oligomers with an even number of repeat units. One possible interpretation is that, during the first step of synthesis of PBT, dimers are overwhelmingly more than trimers. This phenomenon is very singular, in fact no conformational constraints is expected in so large rings. Nevertheless, according to Burzin and Frenzel [17], during the first step of the synthesis of poly(1,4-butylene terephthalate), dimers and trimers are formed with the same probability. At present, we have no explanation for this apparent overestimation of cyclic oligomers production.

### 3.1. Thermo-oxidation processes

In Fig. 3 is shown the MALDI mass spectrum, together with an expanded portion spanning over 220 Da (PBT repeat unit), of a PBT

film sample thermo-oxidized for 15 min at 250 °C. From the inspection of the spectrum a reduction of the molecular masses and the occurrence of ions not detected in the MALDI mass spectrum of the original sample shown in Fig. 2 are evident. This indicates that thermo-oxidation reactions have occurred, producing new compounds that are revealed and differentiated by the MALDI analysis. The favorable event here is that the MALDI spectrum shows many new well-resolved peaks, which provide potential information on the structure and end groups of the oxidation products. All the peaks correspond to PBT oligomers with different end groups and they have been assigned to specific oligomer structures (Table 1). In the MALDI mass spectrum reported in Fig. 3, species bearing 1,4-butane-diol at one end and terephthalic acid groups at the other end (species C, Table 1) are still present, on the contrary the cyclic oligomers (species A at  $m/z$  1344) as well as the oligomers I (1,4-butane-diol end groups at both chain ends, Table 1) are no longer detected. The most abundant ions have been assigned to sodiated linear chains terminated with terephthalic acid at both chain ends (species N Na<sup>+</sup> at  $m/z$  1289; N K<sup>+</sup> at  $m/z$  1305, and the corresponding sodium and potassium salts at  $m/z$  1311, 1333, 1327 and 1349). It is possible to notice the appearance of a new peak at  $m/z$  1375 (species D Na<sup>+</sup> and the corresponding sodium salt at  $m/z$  1397), assigned to sodiated ions of linear oligomers terminated with terephthalic acid at one end and 4-hydroxy butanoic acid at the other end, originated by oxidation of polymer chains. In fact, these species are diagnostic for the occurrence of a  $\alpha$ -H abstraction process (Scheme 1, route 1). The initial step in this process consists in a hydrogen abstraction from the methylene group adjacent to the ester linkage, leading then to the formation of a hydroperoxide intermediate. The latter decomposes to a more stable radical (I) which may follow two different pathways (Scheme 1). The first step of the route 1 cleavage reaction (Scheme 1) yields oligomers terminated with terephthalic acid and 4-hydroxy butanoic acid. Fig. 3 also reveals the presence of ions at  $m/z$  1261 (species L, Table 1) univocally assigned to oligomers with terephthalic acid at one end and phenol groups at the other end. The existence of the phenol terminal groups may be justified by a decarboxylation reaction from the terephthalic acid radical (II) in Scheme 1, route 1.

In addition, in Fig. 3 ions at  $m/z$  1275 (species M and the related sodium salts M<sub>1</sub>, M<sub>2</sub> and M<sub>3</sub>, respectively, at  $m/z$  1297, 1319 and 1341, Table 1) have been univocally identified as chains bearing terephthalic acid at both ends and biphenyl moiety along the polymer chain:



The formation of these species is in agreement with data reported in the literature for aromatic polymers [2,3,12]. In fact, according to previous studies [12] a second oxidation process could be observed in PBT thermo-oxidation. It should be related to crosslinking reactions that in the first step create biphenyl bridges most likely originated from the oxidative coupling of two phenyl

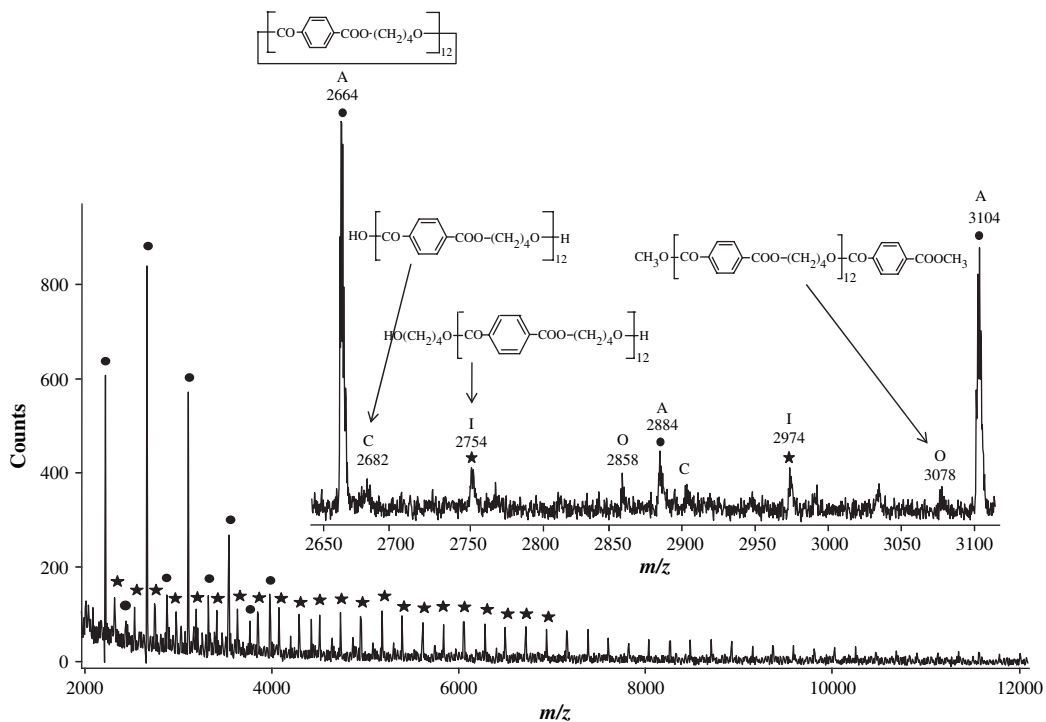


Fig. 2. MALDI-TOF mass spectrum in reflectron mode of the original PBT sample, together with an expanded portion in the  $m/z$  range 2650–3120.

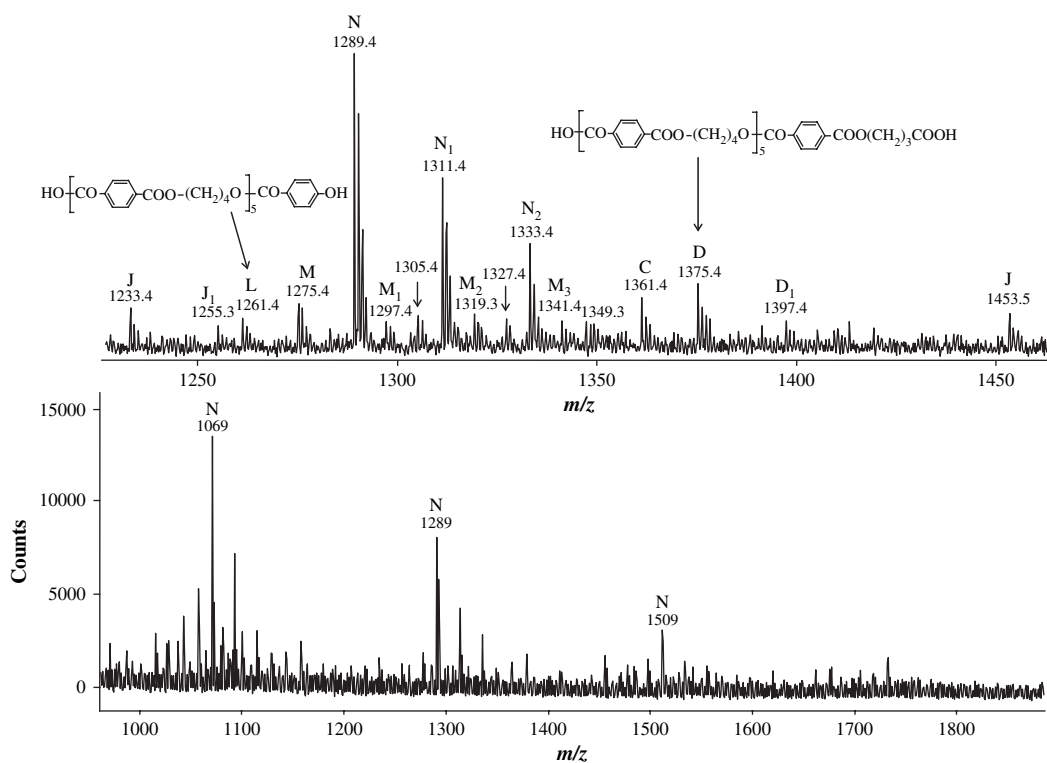
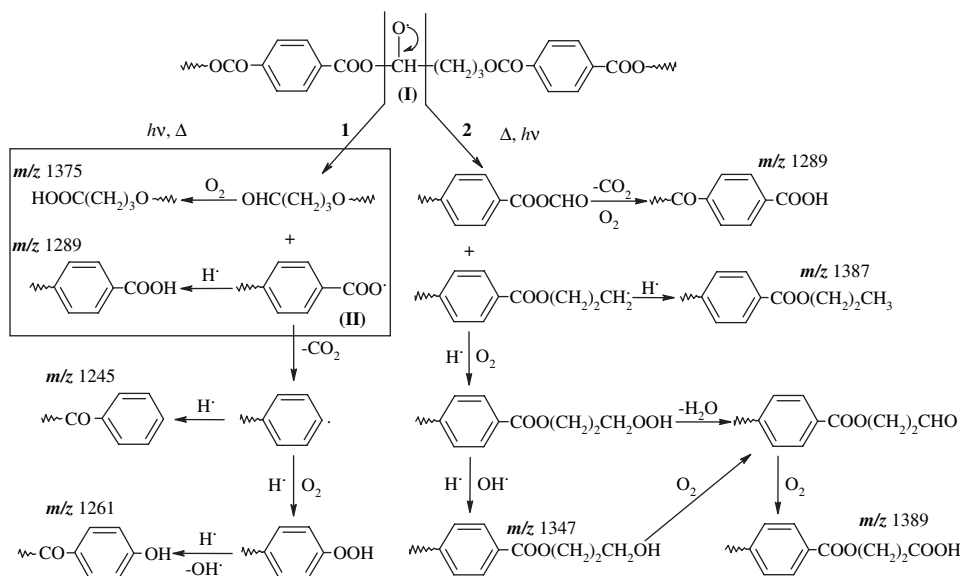
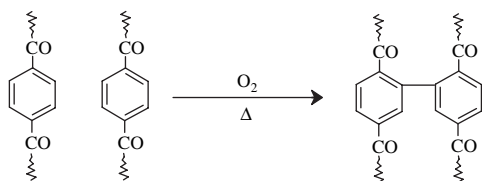


Fig. 3. MALDI-TOF mass spectrum in reflectron mode of a PBT sample thermo-oxidized at 250 °C for 15 min, together with an expanded portion in the  $m/z$  range 1230–1460.



Scheme 1.  $\alpha$ -H hydrogen abstraction mechanism.

rings between linear PBT chains. This reaction promotes the production of cross-linked structures and the gel formation during the thermo-oxidative process.



The structural identification in Table 1 was mainly made on the basis of molecular mass, thus the biphenyl bridges may be linked to any phenyl ring along the polymer chain. In Table 1 we have just symbolized one of the possible structures.

Finally, in the MALDI mass spectrum reported in Fig. 3, ions at  $m/z$  1233 and 1453 (species J, Table 1) can be tentatively assigned to three isobaric structures having butanoic acid/propionic aldehyde as chain ends and/or phenol end groups at both ends and/or oligomers terminated with terephthalic acid at both chain ends with biphenyl groups along the polymer chain (Table 1). The latter assigned structure, bearing three carboxylic groups, is supported by the occurrence of ions at  $m/z$  1255, 1277 and 1299 (species J<sub>1</sub>, J<sub>2</sub>, J<sub>3</sub>, Table 1), unambiguously assigned to the related sodium salt, appearing in the MALDI mass spectra of film samples thermo-oxidized for longer heating times.

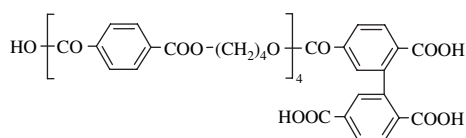


Fig. 4 displays the MALDI-TOF mass spectrum in the  $m/z$  range 1220–1460 of a PBT sample thermo-oxidized for 60 min at 280 °C (a) before and (b) after the *deisotoping* procedure. In fact, due to the effect of isotopic resolution, the identity and relative intensity of peaks in Fig. 4a are not easily assessed; therefore in Fig. 4b the spectrum is shown after the *deisotoping* procedure. Fig. 4b reveals

an increased number of peaks with respect to the spectrum of the PBT sample treated at 250 °C in Fig. 3. In addition to the oligomers present in the previous spectrum, new compounds can be identified at  $m/z$  1245, 1347, 1387, 1389 and 1431 (Table 1). Species K at  $m/z$  1245 (Fig. 4a and b), assigned to oligomers with terephthalic acid at one end and a phenyl group at the other end (Table 1), derive from the  $\alpha$ -H abstraction process (Scheme 1, route 1) as a consequence of a decarboxylation reaction from the terephthalic acid radical (II). Fig. 4b shows the presence of ions at  $m/z$  1347 (species B, Table 1), univocally assigned to oligomers terminated with terephthalic acid at one end and *n*-propanol at the other end. The occurrence of a second rearrangement of the  $\alpha$ -CH radical (I), following the reaction mechanism described in Scheme 1 by route 2, explains the existence of the propanol terminal groups. In fact, the route 2 (Scheme 1) implies the formation of anhydride and *n*-butyl radicals as terminal groups. The former product, after loss of CO<sub>2</sub> and subsequent oxidation, yields to terephthalic acid terminal groups (Species M, Table 1). The *n*-butyl radicals may subtract an hydrogen from the bulk to produce butyl end groups (Scheme 1, route 2), or can be oxidized to intermediate hydroperoxide that decomposes leading to the formation of propanol, propanoic aldehyde and 3-hydroxy propionic acid as terminal groups (Scheme 1, route 2).

In the MALDI spectrum of the PBT samples thermo-oxidized at 250 °C oligomers related to route 2 in Scheme 1 are less abundant or not detected at all. Nevertheless, some of these peaks are revealed at longer heating times, and are detected in the MALDI spectra of the PBT samples thermo-oxidized at 280 °C (Fig. 4).

Species E and F ( $m/z$  1387 and 1389, Table 1) as well as species H ( $m/z$  1431, Table 1), appearing in Fig. 4a and b, correspond at least to two isobaric structures (Table 1). Even so, it can be noticed that all the end groups of the isobaric structures assigned to the ions at  $m/z$  1387 and 1389 derive from the reactions reported in Scheme 1, route 2. These oligomers support the occurrence of the rearrangement described in Scheme 1, route 2, even though the poor abundance of these ions suggests that the thermal-oxidative scission takes place preferentially at the  $\alpha$ -CH bond (Scheme 1, route 1).

Furthermore, less abundant ions at  $m/z$  1343 (species A, Table 1) are detected in the MALDI mass spectra of the thermo-oxidized samples at 280 °C. These oligomers were reasonably attributed to linear chains bearing terephthalic acid at one end and butene



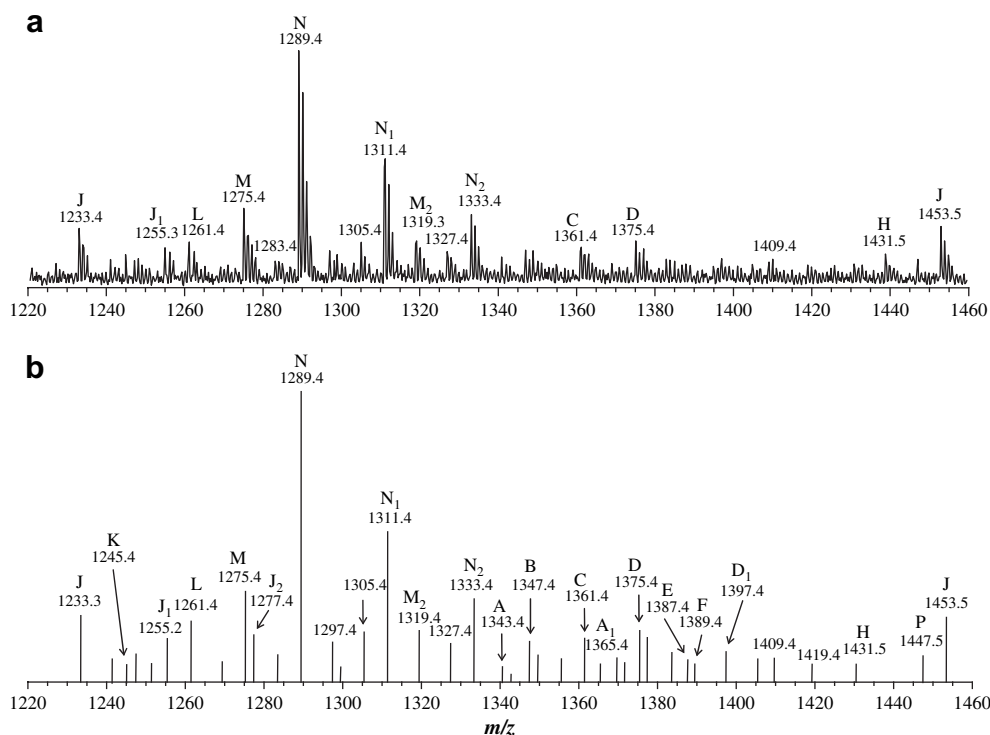
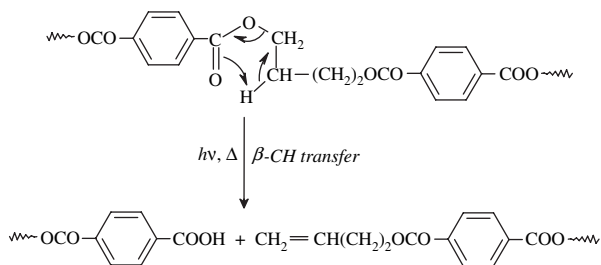


**Fig. 4.** MALDI-TOF mass spectra in *reflectron mode*, in the  $m/z$  range 1220–1460, of a PBT sample thermo-oxidized for 60 min at 280 °C (a) before and (b) after the *deisotoping* procedure.

groups at the other end (Table 1). These species are isobaric with cyclic oligomers (species A, Table 1), but the concurrent presence of ions at  $m/z$  1365, due to the corresponding sodium salts (Species A<sub>1</sub>, Table 1), supports our assignment and suggests that the  $\beta$ -hydrogen transfer [1,7] mechanism (Scheme 2), a thermal degradation process, becomes active at 280 °C. All the mechanisms reported and discussed above are based on the main chain scission. This is reasonable in view of the rapid viscosity decrease. However, the contribution of end group degradation (oxidation, dehydration, decarboxylation) cannot be excluded.



**Scheme 2.**  $\beta$ -Hydrogen transfer mechanism.

### 3.2. Photo-oxidation processes

Fig. 5 shows the MALDI spectrum in the mass range 1270–1460 Da of the PBT sample photo-oxidized at 70 °C for 18 h. The most abundant ions at  $m/z$  1289 (Fig. 5) are due to linear chains terminated with terephthalic acid groups (species N, and the related sodium salts N<sub>1</sub> and N<sub>2</sub>, Table 1). MALDI data reveal also the presence of species at  $m/z$  1375.4 (species D, Table 1) containing 4-hydroxy butanoic acid and terephthalic acid as chain ends. Both these groups derive from a  $\alpha$ -H abstraction process with the consecutive scission at the  $\alpha$ -CH bond (Scheme 1, route 1). Ions at  $m/z$  1361 (species C and the related sodium salt C<sub>1</sub> at  $m/z$  1383) have

been assigned to oligomers terminated with butane-diol and terephthalic acid groups. In Fig. 5 species bearing butane-diol at both chain ends, at  $m/z$  1433 (species I, Table 1), are present as well as sodiated cyclic oligomers at  $m/z$  1343 (species A, Table 1). Fig. 5 also displays abundant ions at  $m/z$  1365. The existence of this peak at 22 mass units from species A (Table 1) implies that product ions at  $m/z$  1343 not only are due to cyclic oligomers but also to sodiated linear chains terminated with an olefin at one end and a terephthalic acid group at the other. In fact, as discussed previously, linear chains bearing terephthalic acid and butene end groups are isobars with cyclic oligomers. Peaks at  $m/z$  1365 due to the corresponding sodium salt of ions at  $m/z$  1343 support our assignment and evidence the occurrence of a  $\beta$ -hydrogen transfer mechanism. Moreover, the detection of less abundant ions at  $m/z$  1415 (species G), assigned to chains with 1,4-butane-diol at one end and butene at the other end, confirm this mechanism. In the literature [2,3], the  $\beta$ -hydrogen transfer promoted by light is inappropriately called Norrish II. In fact, the Norrish II mechanism is a  $\gamma$ -hydrogen transfer. Nevertheless, the  $\beta$ -hydrogen transfer is promoted by pure photolysis action as well as by thermal degradation process at 280 °C.

Ions at  $m/z$  1347 (species B, Table 1), 1389 (species F, Table 1) and 1477 ascertain the occurrence of secondary processes originated from the  $\alpha$ -H abstraction process (Scheme 1, routes 1 and 2). Species F can be assigned to four isobaric structures. One of these structures, bearing a butyl formate end group, could be originated from the Norrish I photo-cleavage but, unfortunately, the occurrence of this reaction cannot be established unambiguously by our mass spectrometric evidence.

Our results are only partially in agreement with the data reported in the literature. In fact, the foregoing studies, focused on the photo-oxidation of PBT [2], report a predominant effect of the photolytic reactions with respect to the photo-oxidative processes. The latter mechanism involves the well known [2]  $\alpha$ -H abstraction process, yielding usually terephthalic and 4-hydroxy butanoic acid. According to the literature, the exclusive photolytic degradation implies at least three processes: (i)  $\beta$ -hydrogen transfer (Norrish II),

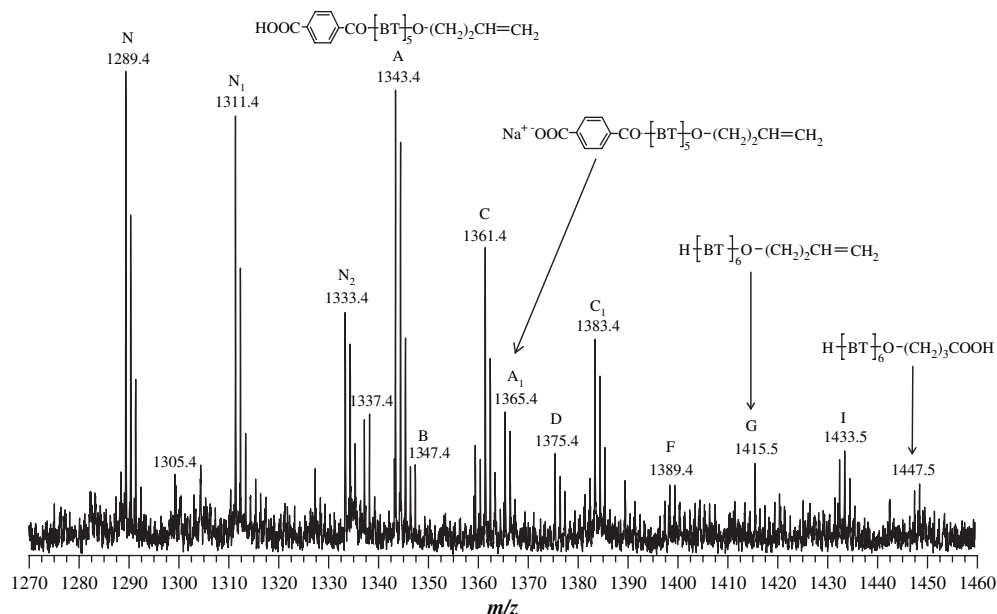


Fig. 5. MALDI-TOF mass spectrum in reflectron mode, in the  $m/z$  range 1270–1460, of a PBT sample photo-oxidized for 18 h at 70 °C (BT =  $-\text{O}(\text{CH}_2)_4\text{OCO}(\text{C}_6\text{H}_4)\text{CO}-$ ).

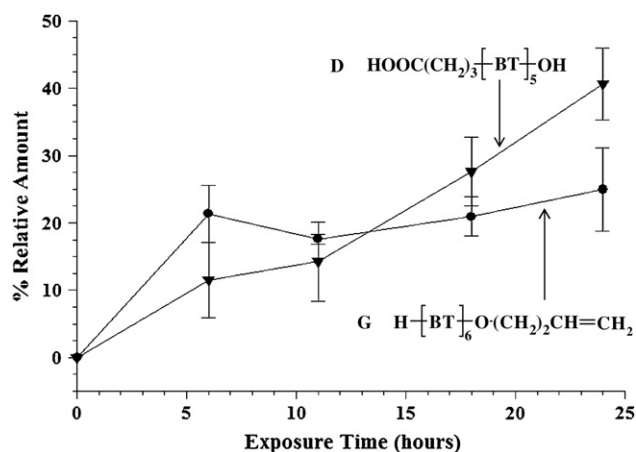


Fig. 6. Intensity profiles of the relative ions abundance vs exposure time of oligomers D and G (Table 1), obtained from the MALDI spectra of the photo-oxidized samples (BT =  $-\text{O}(\text{CH}_2)_4\text{OCO}(\text{C}_6\text{H}_4)\text{CO}-$ ).

(ii) Norrish I cleavage, and (iii) crosslinking reactions through the photolytic coupling of PBT units (Scheme 2).

No evidences of crosslinking reactions were actually found in the MALDI spectra of the photo-oxidized PBT samples.

In Fig. 6 are reported the intensity profiles of the relative ions abundance of two photo-oxidation products representative of the cleavage mechanisms found unambiguously to be operating: the  $\alpha$ -H abstraction and the Norrish II ( $\beta$ -hydrogen transfer) processes. Both the Norrish II photo-product (species G) and the  $\alpha$ -H abstraction photo-oxidation product (species D) are formed immediately and their relative abundance increases with the exposure time. At longer exposure times the  $\alpha$ -H abstraction photo-oxidation (Scheme 1, route 1) becomes prominent.

#### 4. Conclusions

The low sensitivity of characterization techniques in polymer analysis required the support of model compounds in a reduced number of studies concerning the thermo-oxidative degradation of PBT. In this work we have studied the thermal- and photo-oxidation of

a PBT sample by using the highly sensitive MALDI-TOF MS instrument. The structural analysis of the oxidation products provided by MALDI allowed construction of an exhaustive scheme of the thermal- and photo-oxidation mechanisms of poly(1,4-butylene terephthalate). We have partially confirmed and extended the knowledge on thermo- and photo-oxidation mechanisms of PBT. According to the structure of the major oxidation products detected by MALDI (Scheme 1), two thermo-oxidation processes and two photo-oxidation cleavages have been unambiguously ascertained to occur in PBT.

A  $\alpha$ -H hydrogen abstraction mechanism contributes to both the photo- and thermal-oxidation of PBT at 250 and 280 °C, leading to the formation of similar series of oligomers discriminated by MALDI. In fact, the extraction of a methyl hydrogen, yielding a methylene radical which reacts with oxygen to form a hydroperoxide intermediate (Scheme 1) activates both the photo and thermal processes. The decomposition of this hydroperoxide, when occurring thermally at 250 and 280 °C, leads straightforwardly to all the end groups represented in Scheme 1 (routes 1 and 2). On the other hand, the photo-oxidation, performed at 70 °C, is more selective, and the oxidation products bearing phenyl and phenol end groups, derived from loss of  $\text{CO}_2$ , are not observed (Scheme 2, route 1). Despite the data reported in the literature [2–5], our results gives evidence that the  $\alpha$ -H hydrogen abstraction plays an important role in the photo-oxidative degradation process and becomes the prominent mechanism at higher exposure times. Furthermore, MALDI mass spectra support a specific thermo-oxidative pathway: the oxidative coupling of phenyl rings that create biphenyl bridges between PBT chains. This reaction produces cross-linked structures that escaped in previous studies.

Additionally, the inspection of the data acquired by MALDI allowed discriminating the degradation mechanisms entirely induced by light or heat without the involvement of oxygen. In fact, the well known  $\beta$ -hydrogen transfer [4,7] is promoted by pure photolysis action (Norrish II) as well as by pure thermal degradation process at 280 °C (Scheme 2).

#### Acknowledgment

Partial financial support from the Italian Ministry for University and for Scientific and Technological Research and from the National

Council of Research (CNR, Rome) is gratefully acknowledged. The active collaboration of Dr. S. Sgrò, Dr. L. Ferreri and Mr. F. Ferrini to this work is acknowledged.

## References

- [1] Samperi F, Puglisi C, Alicata R, Montaudo G. *Polym Degrad Stab* 2004;83:11–7.
- [2] Rivaton A, Gardette JL. *Die Angew Makromol Chem* 1998;261/262:173–88.
- [3] Rivaton A. *Polym Degrad Stab* 1993;41:283–96.
- [4] Manabe N, Yokata Y. *Polym Degrad Stab* 2000;69:183–90.
- [5] Tabakia MH, Gardette JL. *Polym Degrad Stab* 1986;14:351–65.
- [6] Bothelho G, Queiros A, Liberal S, Gijsman P. *Polym Degrad Stab* 2001;74:39–48.
- [7] Buxbaum LH. *Angew Chem Int Ed Engl* 1968;7:182–6.
- [8] Montaudo G, Samperi F, Montaudo MS. *Prog Polym Sci* 2006;31:277–357.
- [9] Peacock PM, McEwen CN. *Anal Chem* 2006;78:3957–64.
- [10] Carroccio S, Samperi F, Puglisi C, Montaudo G. *Macromolecules* 1999;32:8821–8.
- [11] Chionna D, Puglisi C, Samperi F, Turturro A, Montaudo G. *Macromol Rapid Commun* 2001;22:524–9.
- [12] Carroccio S, Puglisi C, Montaudo G. *Macromolecules* 2002;35:4297–305.
- [13] Carroccio S, Rizzarelli P, Gallet G, Karlsson S. *Polymer* 2002;43:1081–94.
- [14] Carroccio S, Puglisi C, Montaudo G. *Macromolecules* 2003;36:7499–507.
- [15] Carroccio S, Puglisi C, Montaudo G. *Macromolecules* 2004;37:6037–49.
- [16] Carroccio S, Rizzarelli P, Puglisi C, Montaudo G. *Macromolecules* 2004;37:6576–86.
- [17] Burzin K, Frenzel PJ. *Die Angew Makromol Chem* 1978;71:61–6.